Journal of Applied Fluid Mechanics, Vol. 17, No. 11, pp. 2377-2389, 2024.
Available online at www.jafmonline.net, ISSN 1735-3572, EISSN 1735-3645.
https://doi.org/10.47176/jafm.17.11.2601

Numerical Investigation of Flow Inside a Channel with Elastic Vortex Generator and Elastic Wall for Heat Transfer Enhancement

A. A. Abdalrazak Obaid†, S. E. Razavi and F. Talati

Faculty of Mechanical Engineering, University of Tabriz, Tabriz, Iran

†*Corresponding Author Email: ali.assim@tabrizu.ac.ir*

ABSTRACT

In the present investigation, a detailed numerical investigation of the flow and heat transfer characteristics of a channel with an elastic fin (vortex generator) and an elastic wall has been carried out using finite element method. The Fluid-Structure Interaction (FSI) model is used to capture the interaction between the fluid and the solid structure. A sinusoidal time dependent velocity profile has been imposed at the inlet of the channel and the right half of the upper wall of the channel is heated and exposed to constant temperature boundary condition. Due to the sinusoidal velocity profile at the inlet, the elastic fin oscillates periodically and act as a vortex generator, which causes more turbulence in the flow. The obtained results showed that the Nusselt number over the heated wall is affected by the position of the flexible fin, height of flexible fin and elasticity modulus of elastic fin. Moreover, due to the elasticity of the elastic wall and sinusoidal behavior of the inlet velocity, the elastic wall oscillates periodically upward and downward. The Nusselt number values over the heated wall are increased with decrease of the elastic modulus value of the elastic wall. However, the decrease in elastic modulus value of the elastic wall contributes to an increase in the pressure drop inside the channel. It should be added that the interplay between the fluid motion and the deformable structures leads to enhanced turbulence, as the flexible fin and elastic wall introduce additional disturbances and fluctuations into the flow regime. Consequently, this heightened turbulence level has profound implications for heat transfer processes within the system.

Article History

Received January 17, 2024
Revised May 9, 2024
Accepted May 14, 2024
Available online September 1, 2024

Keywords:

Fluid-structure interaction
Elastic wall
Vortex generator
Heat transfer
Flexible fin

1. INTRODUCTION

Heat transfer (HT) enhancement in channels has been an important research topic in recent years due to its significant impact on the efficiency of many industrial processes. Different methods have been proposed to improve the heat transfer rate in channels, including the use of fins, ribs, and swirl generators. Among these methods, the use of flexible fins and elastic walls has shown promising results in enhancing heat transfer while reducing pressure drop. The present study aims to investigate the flow and heat transfer characteristics of a channel equipped with an elastic fin and an elastic wall. Recent investigations in the literature have shown that the use of flexible fins and elastic walls can significantly enhance heat transfer in channels. Mirzaee et al. (2012) presented a heat transfer system that utilizes a single, wall-mounted flexible flag located on the bottom wall, with a fixed bending stiffness. They demonstrated that this system outperforms a system with a wall-mounted rigid flag in terms of heat transfer performance. Park (2020) investigated how the inclination angle of a flexible flag in the vertical direction and the bending rigidity affects the HT performance of the system. The study found that a flexible flag significantly improves thermal efficiency compared to a rigid flag, due to the generation of vortex structures that promote flow mixing. Lee et al. (2017) demonstrated that a system featuring two flexible flags mounted symmetrically on the top and bottom walls of a channel achieves improved HT and thermal efficiency when compared to a system with rigid flags mounted in the same manner, or to a clean system without any additional apparatuses. Besides, the performance of this system surpassed that of a single wall-mounted flexible flag system, which had identical inclination angle and Reynolds number values. Ali et al. (2015) introduced a HT system featuring four wall-mounted flexible flags positioned in two regions: two symmetrically wall-mounted flags in an upstream region and two asymmetrically wall-mounted flags in a downstream

Nomenclature

U	velocity	λ_L, μ_L	first and second Lame parameters
T	temperature	υ	Poisson's coefficient
E	the elasticity modulus	H	height of the channel
ρ_s	represents the density	x	locations of the flexible fin from the inlet
P	pressure	FSI	Fluid-Structure Interaction
μ	dynamic viscosity	Nu	Nusselt number
$\bar{\bar{\sigma}}$	Cauchy stress tensor	T_{in}	inlet temperature

region. The flags were set at a fixed inclination angle of 150°. Their study revealed that as a result of constructive interference between the vortices shed from the upstream flags and those produced by the downstream flags, the flapping amplitude of the downstream flags is increased. With an increase in the flapping amplitude, intense fluid mixing was induced, which hindered the growth of the thermal boundary layer, leading to an increase in the overall heat transfer rate for the flexible flags compared to a rigid case.

Dadvand et al. (2019) conducted a study on heat and mass transfer enhancement techniques using both passive and active methods. A microchannel with a cylindrical obstacle was used, and a flexible beam served as a vortex generator downstream. The oscillation of the beam generated periodic vortices that disrupted the thermal boundary layer, resulting in a significant increase in heat transfer. The flexible beam showed improved performance compared to a rigid beam, with increased heat transfer, decreased friction factor, increased thermal performance, and enhanced mixing. Hosseini et al. (2021) investigated the enhancement of heat transfer and mixing using an elastic vortex generator in a microchannel. The elastic vortex generator, vibrating due to the forces applied by the periodic flow, did not require external power input. Compared to a channel with a rigid vortex generator or no vortex generator, the flapping motion of elastic vortex generator generated sequential vortices that swirled the flow and disrupted the thermal boundary layer, resulting in a 31.4% increase in the Nusselt number and a 14.5% increase in the mixing index. The elastic vortex generator also exhibited lower pressure drop and a 32% increase in the thermohydraulic performance factor, suggesting its potential to enhance the efficiency of heat exchangers, mixers, and reactors. Liao & Jing (2023) conducted a study on fluidic mixing using a Y-shaped elastic flag in a two-dimensional mixer. They found that the flag greatly enhanced mixing at a Reynolds number of 50, with an optimal branched length. However, at Reynolds numbers of 10 and 90, the flag did not improve mixing and instead increased pressure loss. The maximum increase in mixing efficiency was 431.29% at the optimal branched length, with corresponding increases in pressure loss. investigated the flow behavior and heat transfer characteristics in a two-dimensional channel with flexible wings. They examine the influence of Young's modulus of the wings and Reynolds number on flow behavior, heat transfer performance, and the dynamic behavior of the wings. The results reveal three motion modes: deflection, vibration, and flapping. The numerical analysis shows that a higher Young's modulus requires a larger Reynolds number for motion mode transition. The overall performance coefficient (PEC) is used to assess the comprehensive performance, with PEC peaks observed near the rear flexible wing during motion mode transition. In a specific case, PEC increases by up to 1.145 due to the combined effects of front flexible wing blocking and rear flexible wing flapping. Das et al. (2023) conducted a study on heat transfer and pressure drop characteristics in a pulsating channel flow using wall-mounted flexible flow modulators (FFM). The effects of FFM flexibility, orientation angle, and location were investigated using the Galerkin finite element method. Results showed that a single FFM with orientation angle of $\theta = 90°$ offered the best heat transfer enhancement. The study analyzed vorticity contours, isotherms, Nusselt number variations, pressure drop, and power spectrum analysis of thermal field oscillation and FFM motion. Yaseen et al. (2022) examined the mixed convection heat transfer and fluid-structure interaction in a backward-step channel with a flexible step. Various configurations of the flexible step were evaluated to achieve optimal cooling. Results indicated enhancements in the Nusselt number, particularly with a horizontal flexible wall. The Reynolds number had a significant influence on the performance criterion, while the Richardson number did not show a substantial impact.

Ghalambaz et al. (2017) explored the function of a flexible baffle through the use of a thin, highly conductive baffle affixed to one rigid wall of a cavity while leaving the other end free. As a result, the baffle experienced natural convection and fluid stresses. The researchers found that the heat exchange was maximized when the baffle's modulus of elasticity was minimal. Raisi & Arvin (2018) examined the natural convection in a differentially heated cavity that had an elastic top wall and a horizontally fixed elastic baffle located at the cavity center. This particular configuration resulted in a higher Nusselt number compared to a cavity with rigid walls and baffle. Furthermore, their findings demonstrated that the Nusselt number increased as the length of the elastic baffle increased. Soti et al. (2015) investigated heat transfer in the FSI phenomenon in channel flow. They examined the effect of an elastic thin plate attached to the leeward side of a heated rigid cylinder in a channel with laminar flow. The researchers found that the flexible plate had a significant impact on the mixing of fluid by directing the vortices generated near the channel walls into areas of high velocity. This enhanced the heat exchange process and improved the overall efficiency. Sabbar et al. (2018) investigated the heat transfer characteristics of an open cavity that was connected to a parallel-plate channel. The cavity featured a flexible vertical wall that was oriented in the opposite direction to the main flow of the channel. The

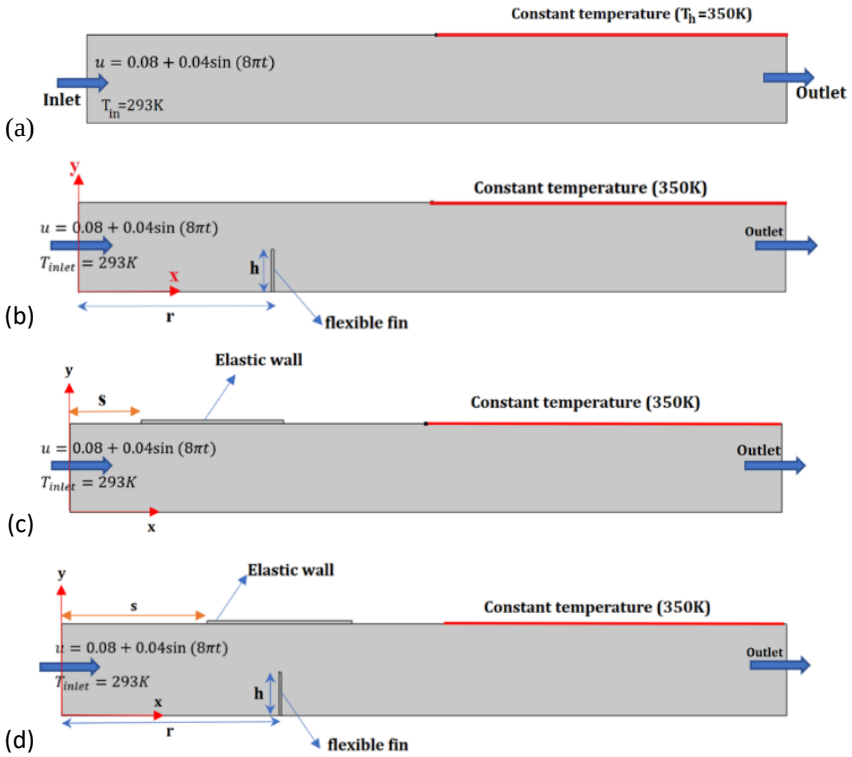

Fig. 1 Schematics of the studied problem: a) without flexible fin and without elastic wall, b) with flexible fin and without elastic wall, c) without flexible fin and with elastic wall, d) with both flexible fin and elastic wall

researchers found that this particular configuration resulted to an increase of 17% in the Nusselt number. Ismael et al. (2022) investigated numerically the thermal performance of a vertical double-passage channel separated by a flexible thin sheet. They found that the use of a flexible separator instead of a rigid separator can passively enhance heat transfer in either passage. However, the flexible sheet was found to increase the pressure drop by up to 200%, which resulted in a decline of the thermal performance criterion to less than one.

Despite the significant progress in the literature, there is still a need for further investigation of the flow and heat transfer characteristics of channels with elastic fins and walls. In this study, we aim to numerically investigate the effect of an elastic fin and an elastic wall on heat transfer and fluid flow in a rectangular channel. The effects of the elasticity and material properties of the fin and wall on the heat transfer rate and pressure drop will be investigated. In summary, the present study aims to contribute to the existing knowledge by providing a detailed numerical investigation of the flow and heat transfer characteristics of a channel with an elastic fin and an elastic wall. The results of this study can be useful for designing more efficient heat exchangers and cooling systems in various industrial applications.

2. PHYSICAL MODEL AND GOVERNING EQUATIONS

2.1 Model Description and Boundary Condition

The schematics of the geometries investigated in the present investigation are shown in Fig. 1. A channel with a flexible fin and elastic wall has been considered. The choice of the specific channel configuration in our investigation was driven by the objective of studying the hydrodynamics and heat transfer characteristics in a system involving both a flexible fin and an elastic wall. The configuration was designed to explore the individual effects of the flexible fin and elastic wall separately, as well as their combined impact on the problem. One potential application of such a configuration is in the field of heat exchangers, where the use of flexible fins and elastic walls can have several advantages. It is worth mentioning, the effect of the exitance of the elastic fin and elastic wall will be investigated separately. Then, the effects of simultaneous use of flexible fin and elastic wall on the hydrodynamics and heat transfer of the problem will be investigated.

The height of the channel is H=25mm. A sinusoidal time dependent velocity profile has been imposed at the inlet of the channel (U=A+Bsin(2πft)) and a uniform temperature of T_{in}=293K has been considered at the channel inlet. The sinusoidal velocity profile serves as a means to simulate and analyze the behavior of the flexible fin and elastic wall under oscillatory flow conditions, which is essential for understanding their individual effects on the hydrodynamics and heat transfer within the channel. The length of the channel is 200mm as well. Different heights of the elastic fins studied in the present study are 8mm, 10mm and 12mm. Different locations of the flexible fin from the inlet of the channel are also x=30mm, 60mm and 90mm. Three different values have also been considered for the elasticity modulus of the elastic fin including $E=10^5$, 10^6 and 10^{22} Pa. The right half of the upper wall is a heated wall which is exposed to

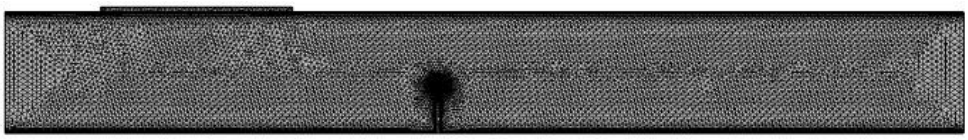

Fig. 2 The used grid

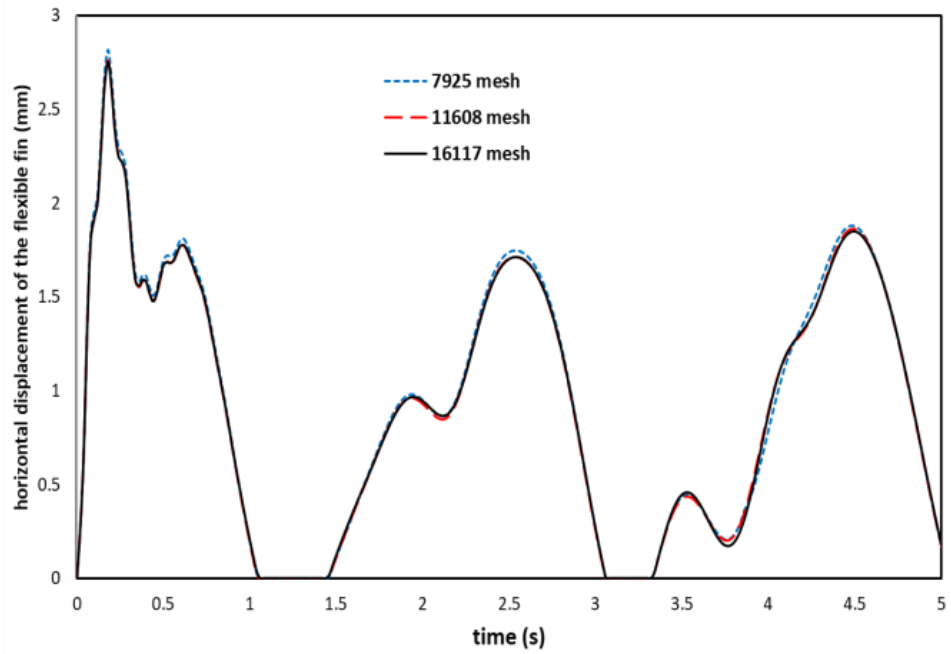

Fig. 3 Variations of the maximum horizontal displacement of the elastic vortex generator (flexible fin) in terms of time for three different grid numbers

constant temperature boundary condition and its temperature is T_h=350K.

2.2 Numerical Method Validation

Figure 2 depicts the mesh used for the computational domain in the present numerical study. As seen, a particular attention has been given to the mesh distribution, especially in regions proximal to the flexible fin and elastic wall. This finer control of mesh density aims to accurately capture the intricate fluid-structure interactions occurring in these critical areas. Besides, a grid independence check of the results from grid number has been carried out. Figure 3 presents the variations of the maximum horizontal displacement of the elastic vortex generator (flexible fin) in terms of time for three different grid numbers of 7925, 11608 and 16117. As seen, with the increase of the grid numbers from 11608 to 16117, the maximum horizontal displacement of the elastic vortex generator does not change considerably. Thus, the grid with mesh number of 11608 is used as our benchmark grid.

The independency of the results from the initial time step size was also investigated. In this regard, three different initial time step size of 0.005s, 0.001s and 0.0005s were considered. It is important to note that the employed software in our analysis is designed to choose a time step smaller than the initial time step size, but it will not increase the time step beyond that value. Finally, it was found that by decreasing the initial time step size from 0.001s to 0.0005s, there was no considerable variations in the obtained results.

In order to check the validity of the numerical method used in the present study, the obtained results have been compared with those of Turek & Hron (2006) which consist of laminar incompressible channel flow around an elastic object which contributes to self-induced oscillations of the structure. As seen in Fig. 4, the variations of the lift force on elastic wall obtained by present numerical method are in good agreement with those of Turek & Hron (2006).

In order to validate the used FSI method, the study conducted by Küttler & Wall (2008) was examined. Their study examined a square cavity with a flexible bottom wall. The top wall of the cavity was subjected to a velocity of (1 - cos(0.4πt)) m/s, while two open gaps were positioned at the top of the vertical walls. The oscillation of the lid caused fluid motion within the enclosure, generating a vortex. Consequently, the interaction between the fluid and the flexible lower wall resulted in changes to the bottom wall's shape. These changes were computed over time. Figure 5 illustrates a comparison between the results based on present numerical method and those of Küttler & Wall (2008) regarding the deformation of the flexible wall after t = 7.5s. The comparison demonstrates a favorable agreement between the results.

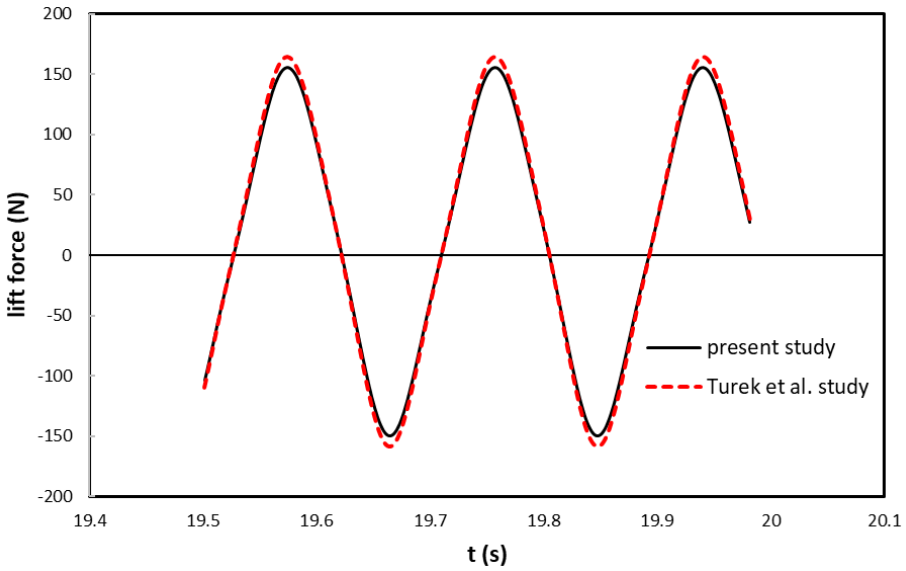

Fig. 4 Variations of the lift force on elastic wall obtained by present numerical method in comparison with those of (Turek & Hron 2006)

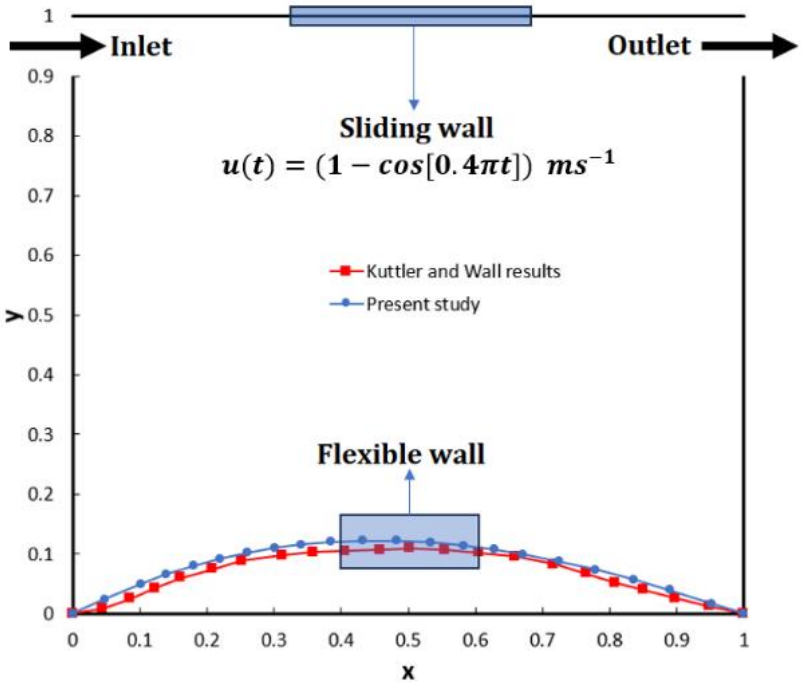

Fig. 5 A comparison between the results based on present numerical method and those of (Küttler & Wall 2008)

2.3 Governing Equations

The continuity equation and momentum equation are (Ali et al., 2016):

$$\nabla.(\vec{u}_f - \vec{u}_m) = 0 \quad (1)$$

$$\frac{\partial \vec{u}_f}{\partial t} + (\vec{u}_f - \vec{u}_m).\nabla\vec{u}_f = -\frac{\nabla P}{\rho_f} + \mu\nabla^2\vec{u}_f \quad (2)$$

where $\vec{u}_f$ denoting the fluid velocity, $\vec{u}_m$and denoting the moving mesh velocity in the fluid domain. The symbols μ, ρ_f, p, and t represent the dynamic viscosity of the liquid, fluid density, pressure, and time, respectively.

The energy equation is as follows (Ali et al., 2016):

$$\frac{\partial}{\partial t}(\rho_f E) + \nabla.\left((\vec{u}_f - \vec{u}_m)(\rho_f E_t + p)\right) = \nabla.(k\nabla T) \quad (3)$$

where E_t is the total energy and k is the thermal conductivity.

The equation of motion of the elastic solid domain is as follows (Lopes et al., 2019):

$$\rho_s \frac{\partial^2 \vec{d}_s}{\partial t^2} - \nabla.\bar{\bar{\sigma}} = \rho_s \vec{b} \quad (4)$$

Density of solid structure×Acceleration of solid structure - Surface forces per volume applied on solid structure =Body forces per volume applied on the solid

In the above equation, ρ_s represents the density of the

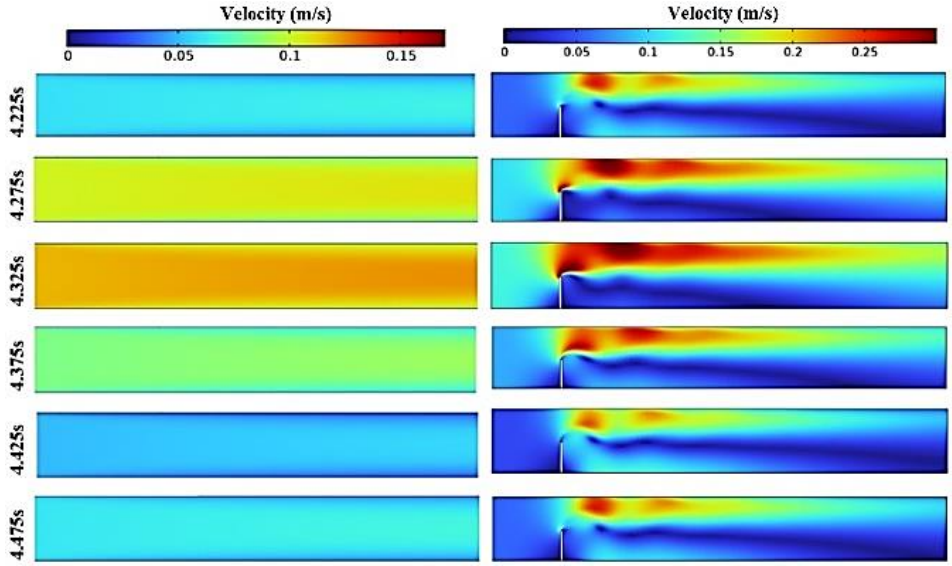

Fig. 6 Variations of the contour of the velocity magnitude inside the channel at different times for the channel without fin and also for the channel with a rigid fin located at r=30mm with the height of 12mm

solid, $\vec{d}_s$ denotes the displacements of the solid, represents the body forces applied on the structure, and $\bar{\bar{\sigma}}$ signifies the Cauchy stress tensor. In the case of an isotropic linear elastic solid, the stress tensor can be expressed as:

$$\bar{\bar{\sigma}} = 2\mu_L \bar{\bar{\varepsilon}} + \lambda_L \, tr(\bar{\bar{\varepsilon}})I \tag{5}$$

In the given equation, λ_L and μ_L represent the first and second Lame parameters, respectively, $\bar{\bar{\varepsilon}}$ denotes the strain tensor, tr signifies the trace function, and I stands for the identity matrix. In the case of compressible materials, the Lame parameters can be expressed as a function of the elastic modulus, E, and Poisson's coefficient, υ (Lopes et al. 2019).

$$\lambda_L = \frac{\upsilon \, E}{(1+\upsilon)(2\upsilon-1)} \tag{6}$$

$$\mu_L = \frac{E}{2(1+\upsilon)} \tag{7}$$

It should be added that the $k-\omega$ turbulence model is used to simulate the turbulent flow within the channel. The $k-\omega$ turbulence model is a widely used two-equation turbulence model that provides accurate predictions of turbulent flow characteristics, including velocity fluctuations and turbulence intensity.

The local Nusselt number is defined as:

$$Nu_{x,t} = -\frac{1}{T_h - T_{inlet}} \left(\frac{\partial T}{\partial n}\right)_{hot\ surface} \tag{8}$$

where (∂T/∂n) is the value of the temperature gradient over the hot surface.

To obtain the spatially-averaged Nusselt number, it is necessary to integrate the local Nusselt number along the hot wall, using the following formula:

$$Nu_t = \frac{1}{L}\int_0^L Nu_{x,t}\,dx \tag{9}$$

$$Nu_x = \frac{1}{t}\int_0^t Nu_{x,t}\,dt \tag{10}$$

3. RESULTS AND DISCUSSION

3.1 Results for the channel with a flexible fin

Figure 6 shows the variations of the contour of the velocity magnitude inside the channel at different times for the channel without fin and also for the channel with a rigid fin located at r=30mm with the height of 12mm. It should be noted that the inlet velocity profile is U=0.08+0.04sin(8πt) which is a turbulent sinusoidal flow. As can be seen, due to the sinusoidal nature of the fluid flow at the entrance of the channel, the distribution of velocity inside the channel varies with time. In the presence of the rigid fin, as can be seen, the fluid flow is deflected due to the collision with the fin, which affects the hydrodynamics and heat transfer of the flow.

Figure 7 also shows the variations of the velocity magnitude contour inside the channel in the presence of a flexible fin with different elastic modulus values. As can be seen, due to the interaction between the fluid and the fin structure, the flexible fin is deformed. Moreover, due to the sinusoidal velocity profile at the inlet, the elastic fin oscillates periodically and act as a vortex generator, which causes more turbulence in the flow. In addition, with the decrease of E value, the fin shows more flexibility against the fluid flow and as a result, the displacement of the fin increases.

Figure 8 depicts the time averaged variations of the local Nusselt number along the length of the heated wall for the channel with flexible fin located at different positions inside the channel including r=30mm, 60mm and 90mm. Figure 9 also shows the temporal variations of space-averaged Nusselt number over the heated wall for different positions of flexible fin. As seen, the existence of flexible has enhanced the heat transfer inside the channel considerably in comparison with no fin case. Besides, the Nusselt number has also been considerably affected by the position of the flexible fin. It is observed that as the distance of the flexible fin situated at the lower wall of the channel decreases from the heated wall, the Nusselt

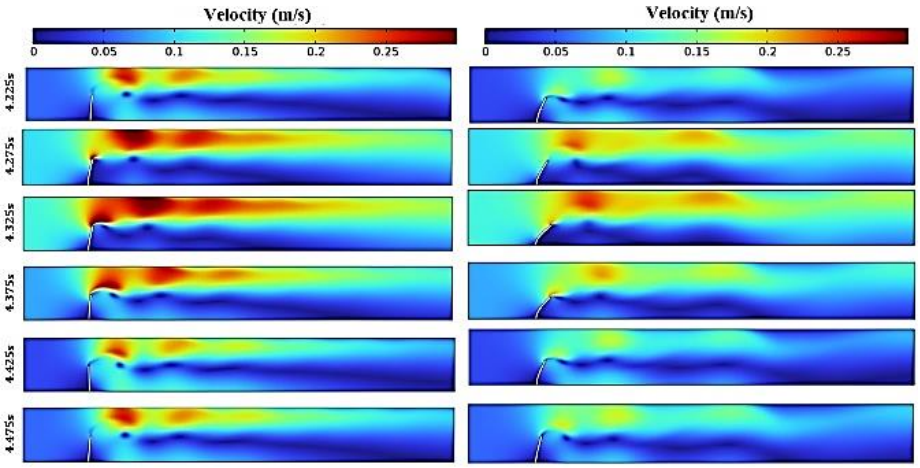

Fig. 7 Velocity contours at different times inside the channel in the presence of a flexible fin with different elastic modulus values of E=1e6 Pa (left side) and E=1e5 Pa (right side)

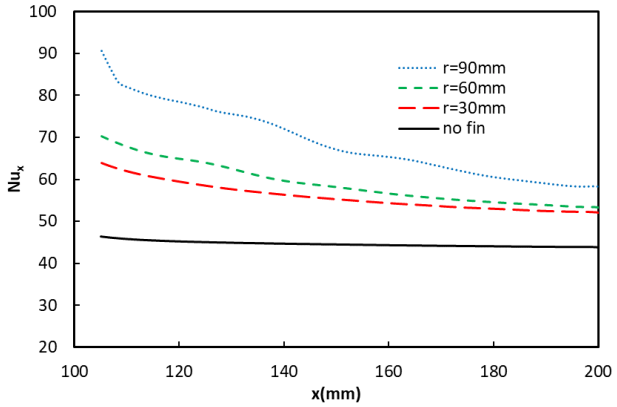

Fig. 8 Time averaged variations of the local Nusselt number along the length of the heated wall for the channel with flexible fin located at different positions of r=30mm, 60mm and 90mm

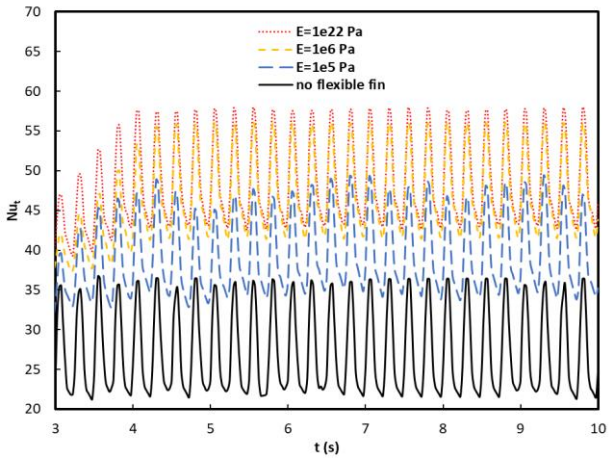

Fig. 10 Effect of the elasticity modulus (E) of the flexible fin located at r=30mm and h=12mm on the temporal variations of space-averaged Nusselt number over the heated wall

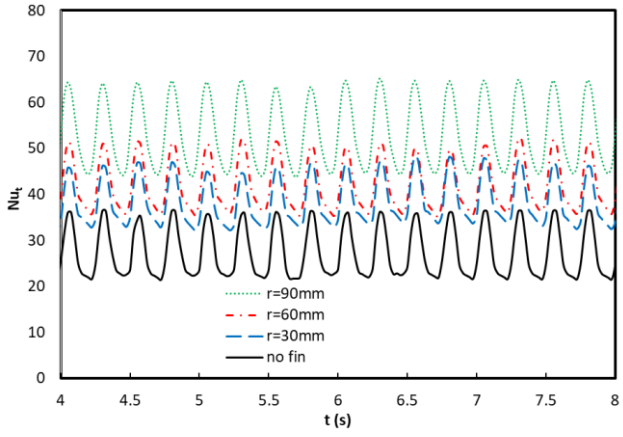

Fig. 9 Temporal variations of space-averaged Nusselt number over the heated wall for different positions of flexible fin

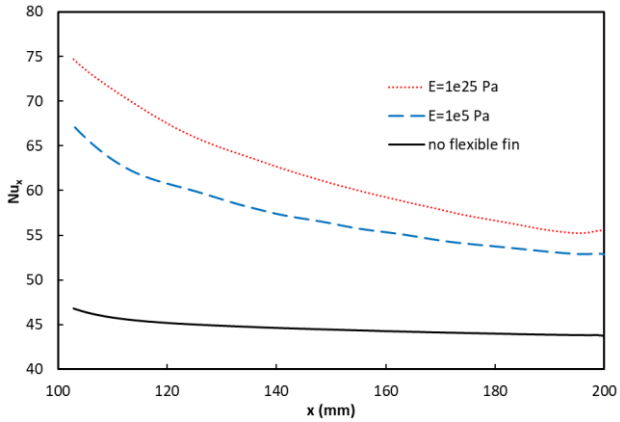

Fig. 11 Time averaged variations of the local Nusselt number along the length of the heated wall for different values of elastic modulus of the flexible fin located at r=30mm and with the height of h=12mm

number is increased and the heat transfer between the fluid flow and the heated wall is enhanced.

Figure 10 shows the effect of the elasticity modulus (E) of the flexible fin located at r=30mm and h=12mm on the temporal variations of space-averaged Nusselt number over the heated wall. Figure 11 also depicts the time averaged variations of the local Nusselt number along the length of the heated wall for different values of elastic modulus of the flexible fin located at r=30mm and

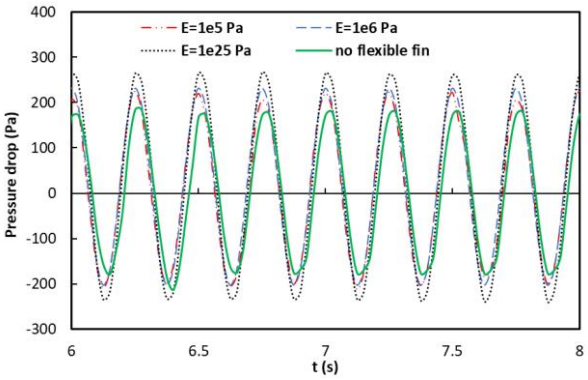

Fig. 12 Temporal variations of the pressure drop inside the channel with a flexible fin with different elastic modulus values and located at r=30m

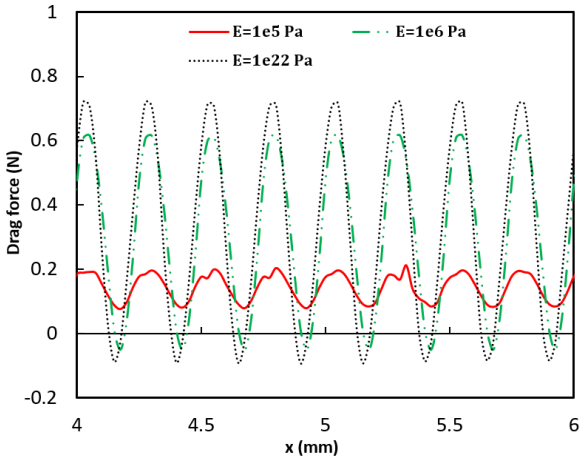

Fig. 13 Temporal variations of the drag force over the flexible fin with different elastic modulus values

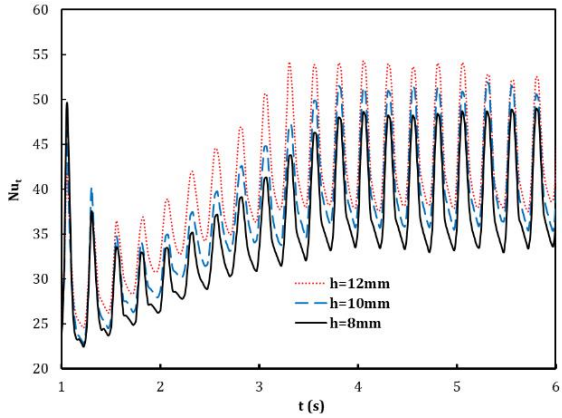

Fig. 14 Influence of the height of the flexible fin with elastic modulus of E=1e5 pa located at r=60mm on the temporal variations of space-averaged Nusselt number

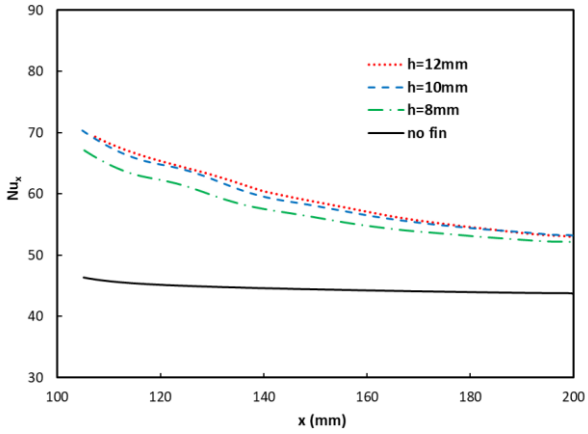

Fig. 15 Time averaged variations of the local Nusselt number along the length of the heated wall for different height values of the flexible fin

h=12mm. As seen, the space averaged Nusselt number has the highest values for the channel with rigid fin (E=1e22 Pa) and the lowest values for the channel with no fin. Moreover, it is seen that with the decrease of the elasticity modulus of the flexible fin, the Nusselt number has been decreased. This is due to the decrease of the velocity magnitude in the vicinity for the heated wall in the existence of flexible fin with lower elastic modulus. It should be mentioned that although the flexible fin with lower elastic modulus act as better vortex generator but it also contributes to lower velocity magnitude near the heated wall in comparison with a flexible fin with higher elastic modulus.

Figure 12 shows the effect of the elastic modulus of the flexible fin on temporal variations of the pressure drop inside the channel with a flexible fin located at r=30mm and with the height of h=12mm. As seen, the pressure drop values have been decreased with decrease of the elasticity value (E) of the flexible fin. This is due to the lower drag force over the flexible fin with lower elastic modulus which is apparently seen in Fig. 13.

Figure 14 depict the influence of the height of the flexible fin with elastic modulus of (E=1e5 Pa) located at r=60mm on the temporal variations of space-averaged Nusselt number over the heated wall. Figure 15 also shows the time averaged variations of the local Nusselt number along the length of the heated wall for different height values of the flexible fin. As seen, the Nusselt number has been increased with increase of the height of flexible fin which denotes better heat transfer from the heated wall.

3.2 Results for the Existence of the Elastic Wall Inside the Channel

In this section, the effect of the existence of an elastic wall over the top wall of the channel on the hydrodynamics and heat transfer of the flow inside the channel will be studied. The length of the elastic wall is 40mm. Figure 16 shows the velocity magnitude contours at different times for the channel including an elastic wall with elastic modulus of (E= 1e6 pa) and s=40mm. As seen, due to the elasticity of the elastic wall and sinusoidal behavior of the inlet velocity, the elastic wall oscillates periodically upward and downward. Thus, the fluid flow through the channel is totally affected by the oscillation of the elastic wall and it becomes more turbulent.

Figure 17 depicts the influence of the elastic modulus value (E) of the elastic wall on the temporal variations of space-averaged Nusselt number at s=60mm. Moreover, Fig. 18 shows the effect of the increase of the elastic modulus value (E) of the elastic wall on the time averaged variations of the local Nusselt number along the length of the heated wall (s=60mm). As seen in these figures, the

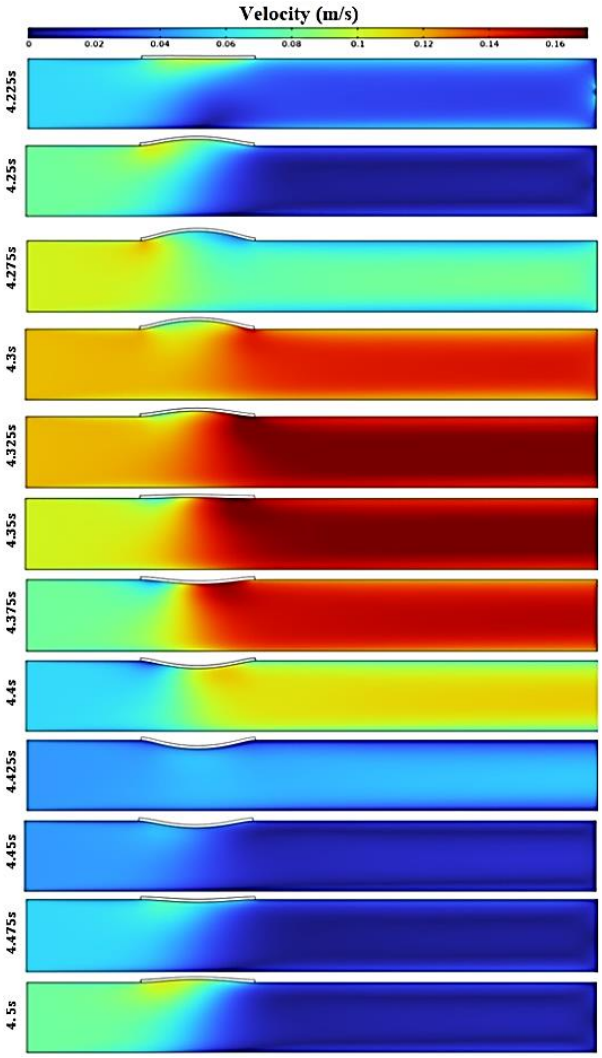

Fig. 16 Velocity magnitude contours at different times for the channel including an elastic wall with elastic modulus of E= 1e6 Pa and s=40mm

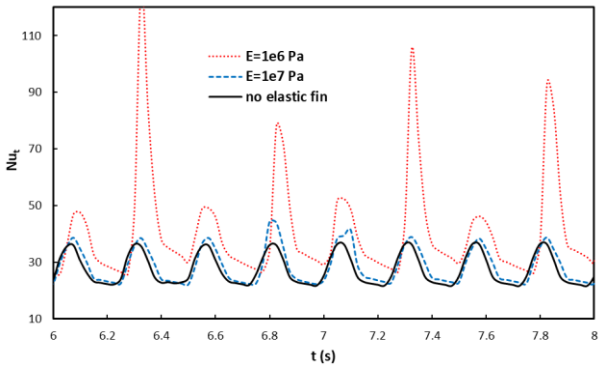

Fig. 17 Influence of the elastic modulus value (E) of the elastic wall on the temporal variations of space-averaged Nusselt number at s=60mm

Nusselt number values are increased with decrease of the elastic modulus value of the elastic wall. Thus, unlike the flexible fin, the decrease of the elastic modulus of the elastic wall contributes to better HT between the fluid flow and the heated wall.

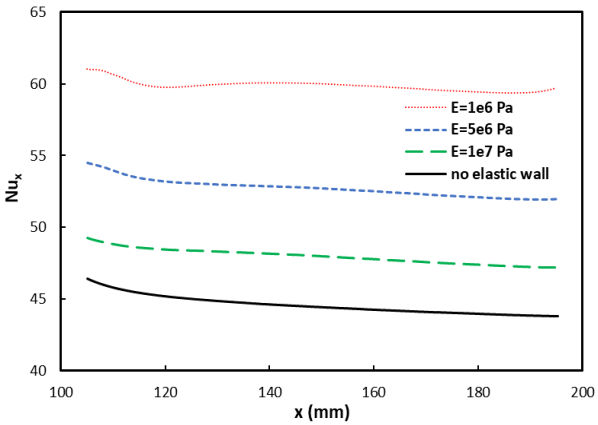

Fig. 18 Effect of the increase of the elastic modulus value (E) of the elastic wall on the time averaged variations of the local Nusselt number along the length of the heated wall (s=60mm)

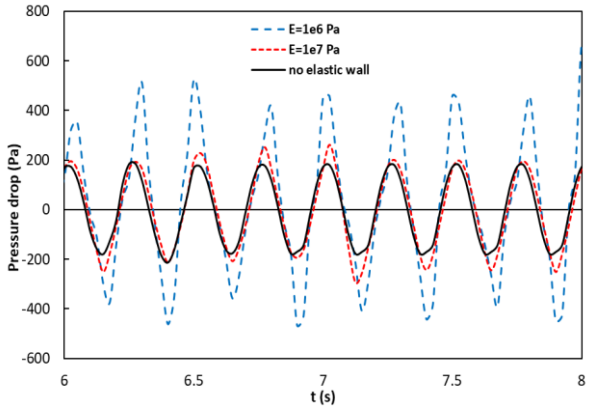

Fig. 19 Influence of the elastic modulus value (E) of the elastic wall on the temporal variations of the pressure drop inside the channel including an elastic wall with s=60mm

The influence of the elastic modulus value (E) of the elastic wall on the temporal variations of the pressure drop inside the channel including an elastic wall with s=60mm has been depicted in Fig. 19. It is found that although the increase in the elastic modulus of the elastic wall improves the HT, but as can be seen in this figure, the increase in elastic modulus has been contributed to decrease in the pressure drop inside the channel

The effect of the position of the elastic wall on the HT over the heated wall has also been studied. Figure 20 depicts the time averaged variations of the local Nusselt number along the length of the heated wall (E=1e6 Pa) for different position of the elastic wall (s=20mm, 40mm, 60mm). As seen, with increase of the increase of the distance of elastic wall from the heated wall (decrease of s value), the Nusselt number and HT have been enhanced. The existence of the elastic wall at distances close to the heated wall leads to the collision of the fluid flow with the oscillating elastic wall and its deflection from its path. Thus, the fluid flow will be in a weak contact with the heated wall which contributes to weak HT.

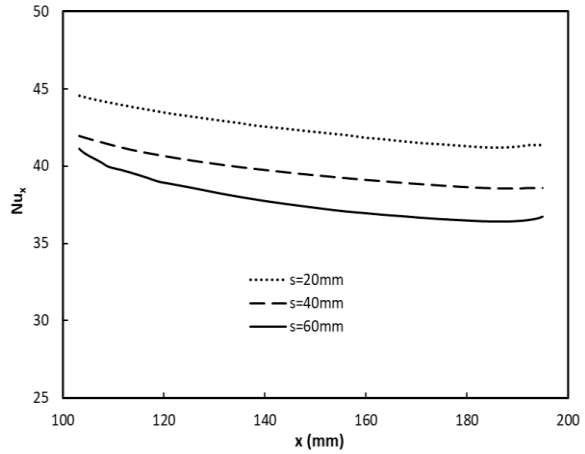

Fig. 20 Time averaged variations of the local Nusselt number along the length of the heated wall (E=1e6 Pa) for different position of the elastic wall (s=20mm, 40mm, 60mm)

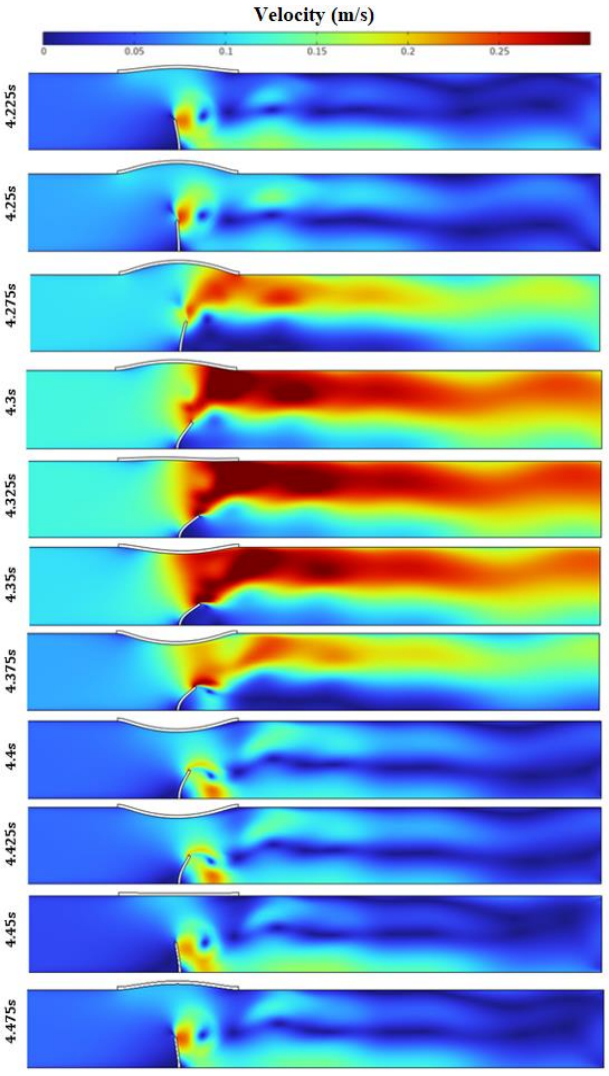

Fig. 21 Velocity magnitude contours at different times for the channel including both flexible fin (E=1e5 Pa, r=60mm and h=10mm) and elastic wall (E= 1e6 Pa and s=40mm

3.3. Effects of Combination of Flexible Fin and Elastic Wall

In this part, the results of the combination of the flexible fin and the elastic wall on the hydrodynamics and HT of the flow inside the channel with sinusoidal inlet velocity profile will be presented. Figure 21 depicts the velocity magnitude contours at different times for the channel including both flexible fin (EFF=1e5 Pa, r=60mm and h=10mm) and elastic wall (E= 1e6 and s=40mm.

Figure 22 depicts the temporal variations of the contour of turbulent kinetic energy inside the channel with both flexible fin (E=1e5 Pa, h=10mm and r=60mm) and elastic wall (E=1e6 Pa and s=40mm). Turbulent kinetic energy contour provides information about the energy associated with turbulent fluctuations, which is important for understanding the intensity and mixing characteristics of the flow. Higher turbulent kinetic energy values generally indicate higher turbulence levels and can lead to enhanced heat transfer rates. As seen, the existence of flexible fin and elastic wall contributes to higher values of turbulent kinetic energy and higher turbulence level. This elevated turbulence level subsequently enhances heat transfer within the system. The presence of both the flexible fin and the elastic wall significantly influences the turbulence characteristics within the flow field. This influence manifests in heightened levels of turbulent kinetic energy and an overall increase in turbulence intensity. The interplay between the fluid motion and the deformable structures leads to enhanced turbulence, as the flexible fin and elastic wall introduce additional disturbances and fluctuations into the flow regime. Consequently, this heightened turbulence level has profound implications for heat transfer processes within the system. The intensified turbulence promotes more vigorous mixing and greater fluid agitation, thereby augmenting heat transfer rates.

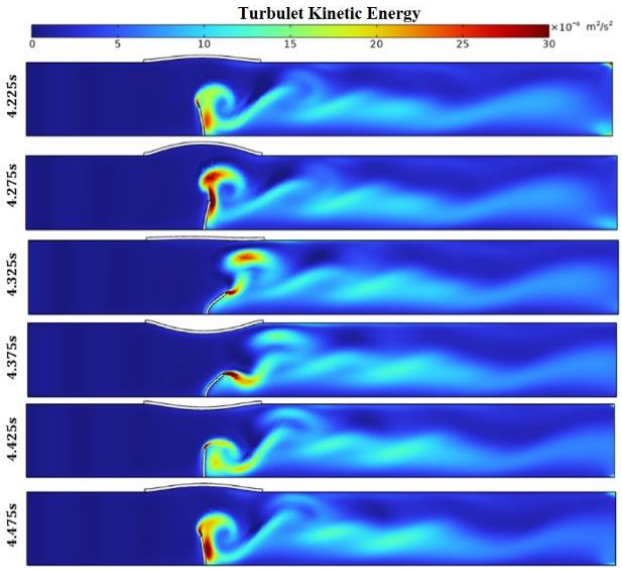

Fig. 22 Temporal variations of the contour of turbulent kinetic energy inside the channel with flexible fin (E=1e5 Pa, h=10mm and r=60mm) and elastic wall (E=1e6 Pa and s=40mm)

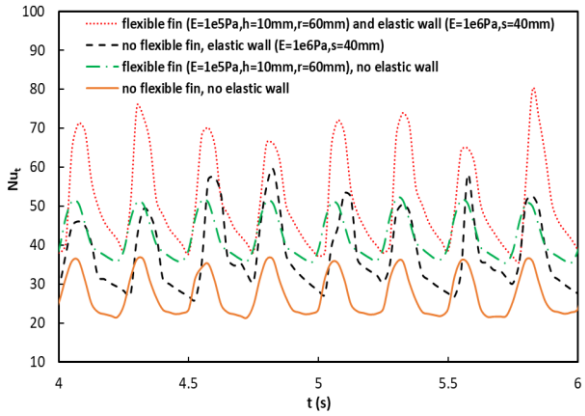

Fig. 23. Temporal variations of space-averaged Nusselt number of the fluid flow for different cases

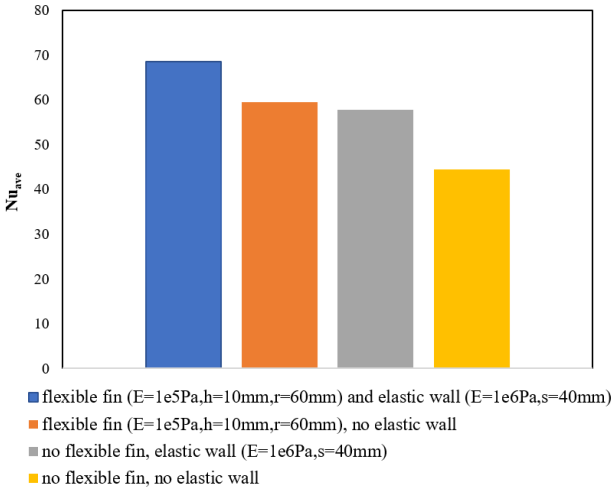

Fig. 24 Total Nusselt number, averaged both temporally and spatially for the fluid flow across different configurations of the channel

Figure 23 depict the temporal variations of space-averaged Nusselt number of the fluid flow for a channel with no elastic fin and no elastic wall, for the channel with a flexible fin (E=1e5 Pa, h=10mm and r=60mm) and no elastic wall, for a channel with an elastic wall (E=1e6 Pa and s=40mm), for a channel including both flexible fin (E=1e5 Pa, h=10mm and r=60mm) and elastic wall (E=1e6 Pa and s=40mm). As seen, the combination of the flexible fin and elastic wall has been contributed to extra considerable enhancement of Nusselt number and HT.

Figure 24 depicts the total (time and spatial averaged) Nu number for the fluid flow inside the channel with no elastic fin and no elastic wall, the channel with flexible fin (E=1e5 Pa, h=10mm and r=60mm) and no elastic wall, the channel with an elastic wall (E=1e6 Pa and s=40mm) and no flexible fin, and for the channel including both flexible fin (E=1e5 Pa, h=10mm and r=60mm) and elastic wall (E=1e6 Pa and s=40mm). Notably, the channel with both the flexible fin and elastic wall exhibits the highest average Nusselt number, followed by the channel solely equipped with the flexible fin. The channel with no elastic fin and no elastic wall has the lowest average Nusselt number value as well.

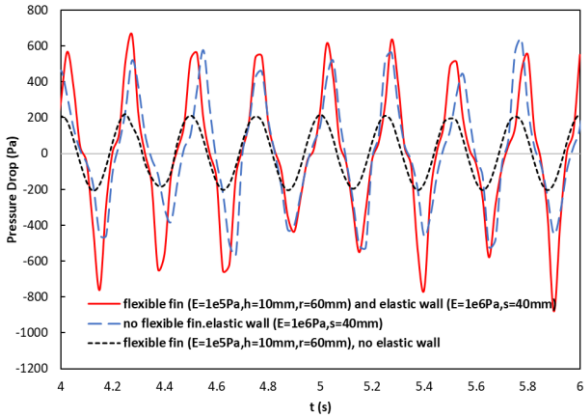

Fig. 25 Temporal variations of pressure drop for different studied cases

Figure 25 also shows the temporal variations of pressure drop for the channel with no elastic fin and no elastic wall, for the channel with a flexible fin (E=1e5 Pa, h=10mm and r=60mm) and no elastic wall, for a channel with an elastic wall (E=1e6 Pa and s=40mm), for a channel including both flexible fin (E=1e5 Pa, h=10mm and r=60mm) and elastic wall (E=1e6 Pa and s=40mm). As seen, utilization of both flexible fin and elastic wall inside the channel has increased the pressure drop inside the channel. However, the increase is not considerable.

In order to evaluate the thermal performance of the channel with flexible fin (E=1e5 Pa, h=10mm and r=60mm) and no elastic wall, the channel with an elastic wall (E=1e6 Pa and s=40mm) and no flexible fin, and the channel including both flexible fin (E=1e5 Pa, h=10mm and r=60mm) and elastic wall (E=1e6 Pa and s=40mm) relative to the thermal performance of a channel lacking both flexible and elastic wall, a metric known as the thermal performance ratio (Webb, 1994) is introduced which is defined which is specified as $(\frac{Nu}{Nu_0})/(\frac{dP}{dP_0})^{1/3}$. Nu_0 and dP_0 corresponds to Nusselt number and pressure drop related to channel with no flexible fin and no elastic wall. Fig. 26 depicts the values of thermal performance ratio for the channel with flexible fin (E=1e5 Pa, h=10mm and r=60mm) and no elastic wall, the channel with an elastic wall (E=1e6 Pa and s=40mm) and no flexible fin, and for the channel including both flexible fin (E=1e5 Pa, h=10mm and r=60mm) and elastic wall (E=1e6 Pa and s=40mm).

4. CONCLUSION

In the present study, a numerical investigation about hydrodynamic and HT of sinusoidal flow inside a channel with an elastic fin (vortex generator) and an elastic wall were conducted using finite element method and the following conclusion were drawn from the present investigation:

- Due to the sinusoidal velocity profile at the inlet, the elastic fin oscillates periodically and act as a vortex generator, which causes more turbulence in the flow.

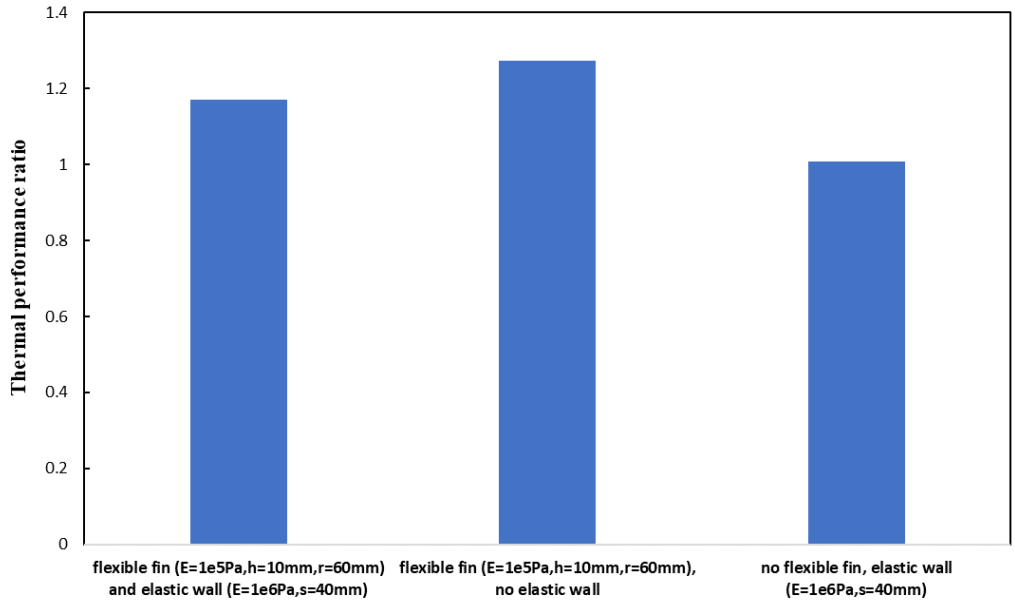

Fig. 26 Values of thermal performance ratio for the channels with different configurations

- The Nusselt number has also been considerably affected by the position of the flexible fin. As the distance of the flexible fin situated at the lower wall of the channel decreases from the heated wall, the Nusselt number is increased and the HT between the fluid flow and the heated wall is enhanced.

- With the decrease of the elasticity modulus od the flexible fin, the Nusselt number decreases due to the decrease of the velocity magnitude in the vicinity for the heated wall. The pressure drop values decreases with decrease of the elasticity value (E) of the flexible fin due to the lower drag force over the flexible fin with lower elastic modulus.

- The Nusselt number increases with increase of the height of flexible fin.

- Due to the elasticity of the elastic wall and sinusoidal behavior of the inlet velocity, the elastic wall oscillates periodically upward and downward

- Unlike the flexible fin, the decrease of the elastic modulus of the elastic wall contributes to better HT between the fluid flow and the heated wall.

- Nusselt number and HT are enhanced over the heated wall with increase of the distance of elastic wall from the heated wall.

- the combination of the both flexible fin and elastic wall contributes to considerable enhancement of Nusselt number and HT while the increase of pressure drop increases trivially.

CONFLICT OF INTEREST

The authors declare that they have no known competing financial interests or personal relationships that could have appeared to influence the work reported in this paper.

AUTHORS CONTRIBUTION

Ali Assim Abdalrazak Obaid: Conceptualization, Data curation, Investigation, Software, Formal analysis, Writing – original draft. equalization, Writing – review & editing, Investigation, Methodology, Resources. **Seyed Esmail Razavi:** Supervision, Conceptualization, Data curation, Resources, Methodology, Validation, Data curation, Writing – review & editing. **F. Talati**: Writing – review & editing.

REFERENCES

Ali, S., Habchi, C., Menanteau, S., Lemenand, T., & Harion, J. L. (2015). Heat transfer and mixing enhancement by free elastic flaps oscillation. *International Journal of Heat and Mass Transfer, 85*, 250-64. https://doi.org/10.1016/j.ijheatmasstransfer.2015.01.122

Ali, S., Menanteau, S., Habchi, C., Lemenand, T., & Harion, J. L. (2016). Heat transfer and mixing enhancement by using multiple freely oscillating flexible vortex generators. *Applied Thermal Engineering*, *105*, 276–89. https://doi.org/10.1016/j.applthermaleng.2016.04.130

Dadvand, A., Hosseini, S., Aghebatandish, S., & Khoo, B. C. (2019). Enhancement of heat and mass transfer in a microchannel via passive oscillation of a flexible vortex generator, *Chemical Engineering Science*, *207*, 556–80. https://doi.org/10.1016/j.ces.2019.06.045

Das, A., Mahmood, F. T., Smriti, R. B., Saha, S., & Hasan, M. N. (2023). CFD analysis of heat transfer enhancement by wall mounted flexible flow modulators in a channel with pulsatile flow, *Heliyon*,

9(6). https://doi.org/10.1016/j.heliyon.2023.e16741

Ghalambaz, M., Jamesahar, E., Ismael, M. A., & Chamkha, A. J. (2017). Fluid-structure interaction study of natural convection heat transfer over a flexible oscillating fin in a square cavity. *International Journal of Thermal Sciences*, *111*, 256–73. https://doi.org/10.1016/j.ijthermalsci.2016.09.001

Hosseini, S., Aghebatandish, S., Dadvand, A., & Khoo, B. C. (2021). An immersed boundary-lattice boltzmann method with multi relaxation time for solving flow-induced vibrations of an elastic vortex generator and its effect on heat transfer and mixing. *Chemical Engineering Journal*, *405*, https://doi.org/10.1016/j.cej.2020.126652

Ismael, M. A., Hussain, S., Alsabery, A. I., Chamkha, A. J., & Hashim, I. (2022, October 1). Thermal performance of a vertical double-passage channel separated by a flexible thin sheet. *International Communications in Heat and Mass Transfer*, *137*, 106238. https://doi.org/10.1016/J.ICHEATMASSTRANSFER.2022.106238

Küttler, U., & Wall, W. A. (2008). Fixed-point fluid-structure interaction solvers with dynamic relaxation. *Computational Mechanics*, *43*(1), 61–72. https://doi.org/10.1007/s00466-008-0255-5

Lee, J. B., Park, S. G., Kim, B., Ryu, J., & Sung, H. J. (2017). Heat transfer enhancement by flexible flags clamped vertically in a poiseuille channel flow. *International Journal of Heat and Mass Transfer*, *107*, 391–402. https://doi.org/10.1016/j.ijheatmasstransfer.2016.11.057

Liao, W., & Jing, D. (2023). Parametric study on the mixing and pressure loss of channel flow behind cylinder connected with y-shaped elastic flag. *Chemical Engineering and Processing - Process Intensification*, *184*, https://doi.org/10.1016/j.cep.2023.109270

Lopes, D., Puga, H., Teixeira, J. C., & Teixeira, S. F. (2019). Influence of arterial mechanical properties on carotid blood flow: comparison of cfd and fsi studies. *International Journal of Mechanical Sciences*, *160*, 209–18. https://doi.org/10.1016/j.ijmecsci.2019.06.029

Mirzaee, H., Dadvand, A., Mirzaee, I., & Shabani, R. (2012). Heat transfer enhancement in microchannels using an elastic vortex generator. *Journal of Enhanced Heat Transfer*, *19*(3), 199–211. https://doi.org/10.1615/JEnhHeatTransf.2012002747

Park, S. G. (2020). Heat transfer enhancement by a wall-mounted flexible vortex generator with an inclination angle. *International Journal of Heat and Mass Transfer*, *148*. https://doi.org/10.1016/j.ijheatmasstransfer.2019.119053

Raisi, A., & Arvin, I. (2018). A numerical study of the effect of fluid-structure interaction on transient natural convection in an air-filled square cavity. *International Journal of Thermal Sciences*, *128*, 1–14. https://doi.org/10.1016/j.ijthermalsci.2018.02.012

Sabbar, W. A., Ismael, M. A., & Almudhaffar, M. (2018). Fluid-structure interaction of mixed convection in a cavity-channel assembly of flexible wall. *International Journal of Mechanical Sciences*, *149*, 73–83. https://doi.org/10.1016/j.ijmecsci.2018.09.041

Soti, A. K., Bhardwaj, R., & Sheridan, J. (2015). Flow-induced deformation of a flexible thin structure as manifestation of heat transfer enhancement. *International Journal of Heat and Mass Transfer*, *84*, 1070–81. https://doi.org/10.1016/j.ijheatmasstransfer.2015.01.048

Turek, S., & Hron, J. (2006). Proposal for numerical benchmarking of fluid-structure interaction between an elastic object and laminar incompressible flow. *Lecture Notes in Computational Science and Engineering*, *53*, 371–85. https://doi.org/10.1007/3-540-34596-5_15

Webb, R. L. (1994). Principles of Enhanced Heat Transfer, 1994. https://doi.org/10.1016/0301-9322(95)90005-5

Yaseen, D. T., Majeed, A. J., & Ismael, M. A. (2022). Cooling of hot cylinder placed in a flexible backward-facing step channel. *Thermal Science and Engineering Progress*, *33*. https://doi.org/10.1016/j.tsep.2022.101364